3

Structure Characterization of Materials by Association of the Raman Spectra and X-Ray Diffraction Data

Luciano H. Chagas[1], Márcia C. De Souza[1], Weberton R. Do Carmo[1], Heitor A. De Abreu[2] and Renata Diniz[1]
[1]*Departamento de Química, Universidade Federal de Juiz de Fora,*
[2]*Departamento de Química, Universidade Federal de Minas Gerais,*
Brazil

1. Introduction

Supramolecular chemistry, which can be described as the chemistry beyond the covalent bonds, has become a very interesting focus of investigation in the last years. The main purpose of this kind of studies is the strategic construction of specific arrangements, and the complete comprehension of the connection between structure and physical–chemical properties. However, in the solid state there are several weak interactions, as hydrogen bonds and π-stacking, which can play a decisive role in orientation of the crystallization processes (Carlucci et al., 2003). Essentially, common features of all of the supramolecular systems are non-covalent interactions, which provide the clips linking the building blocks, leading to well organized superstructures (Yan et al., 2007). The term "Supramolecular chemistry" was introduced by Jean-Marie Lehn and it is defined as "the chemistry beyond the molecule". While a covalent bond normally has a homolytic bond dissociation energy that ranges between 20 and 100 kcal mol^{-1}, noncovalent interactions are generally weak and vary from less than 1 kcal mol^{-1} for van der Waals forces, through approximately 25 kcal mol^{-1} for hydrogen bonds, to 60 kcal mol^{-1} for Coulomb interactions (Hoeben et al., 2005).
In this sense, the most important interactions in solid organic compounds are the hydrogen bonds. The kind and strength of these interactions added to the molecular arrangement are responsible for the crystal structure of these compounds. The change in production and/or storage conditions of solids may modify the hydrogen bonding design and the balance between them and van der Waals interactions. These modifications give rise several changes in the solid state, like phase transitions (Wang et al., 2009). Weak attractive forces are important in deciding the conformation of organic compounds and 3D structure of biomacromolecules. Among molecular interactions, the van der Waals force, electrostatic interactions and hydrogen bonds are the most important (Takahashi et al., 2010).
Apart of hydrogen bonds, another type of interaction that plays an important role in the design of supramolecular materials is π-π interactions. Attractive non-bonded interactions between aromatic rings are seen in many areas of chemistry, and hence are of interest to all realms of chemistry. The strength as well as the causes of these interactions, however, varies. In water the stacking interaction between aromatic molecules is mainly caused by the

hydrophobic effects. Thus, π-π stacking is an important supramolecular force in molecular architecture and recognition. This force is engendered by aromatic–aromatic stacking, which enhances the stability of the complexes both in solution and in solid state. In particular, the π-π stacking interactions in solid state are widely observed in the construction of multi-dimensional structures in offset face-to-face and edge-to-face fashions; combination with coordination bonds, such π stacking interactions can be employed to build up interesting coordination supramolecular architectures (Ye et al., 2005).

The most common effect of modifications in intermolecular interactions in pharmaceutics solids is the polymorphism. Polymorphism is the capacity of the compound to crystalize in two or more different forms. This effect is very important in pharmaceutical science due to the fact that not always all polymorph has the same biodisponibility. These systems will contain drugs which are not in their thermodynamically stable state, and thus need to be stabilized against physical as well as chemical degradation (Aaltonen et al., 2008). Despite of the physical-chemical properties, the investigation of solids in pharmaceutics sciences is important because the solid formulations are the most important pharmaceutical dosage forms, due to the convenience and acceptability of solid oral forms (Aaltonen et al., 2008).

The mainly technic to identify and to investigate these interactions is the X-ray diffraction. However, vibrational spectroscopy can also be used in this kind of characterization, in special in association with crystal data. Raman and IR spectroscopy probe the solid state predominantly on the intramolecular level, although X-ray diffraction predominantly probes the "lattice level", i.e. the intermolecular level (Aaltonen et al., 2008). In addition, the computational study can contribute to the molecular or atomic level understanding the structural and thermodynamical features involved in the process of molecular recognition and supramolecular organization. The combination of these technics provides a complete description of the solid state, in special for crystalline materials. Collaborative studies by both computational and experimental groups are highly encouraged in the supramolecular chemistry (Yan et al., 2007).

2. Hydrogen bonds and vibrational spectroscopy

2.1 Description of hydrogen bonds

The hydrogen bond (or H-bond) is of great importance in natural sciences. This is related particularly to biological aspects, such as molecular recognition that could be a basis for the creation of life. The H-bond is an intermediate range intermolecular interaction between electron-deficient hydrogen and a region of high electron density. Its fundamental role in the structure of DNA and the secondary and tertiary structure of proteins is well known (Kollman and Allen, 1972). In many crystal lattices of organic compounds the H-bonds are a decisive factor governing the molecular packing. In designing of new interesting crystal structures, which is the subject of fast developing crystal engineering, one of the main parameters is the engagement of H-bonds (Sobczyk et al., 2005).

The IUPAC definition is "the hydrogen bond is a form of association between an electronegative atom and a hydrogen atom attached to a second, relatively electronegative atom. Its best considered as an electrostatic interaction heightened by a small size of hydrogen, which permits proximity of interacting dipoles or charges. Both electronegative atoms are usually (but not necessary) from the first row of the Periodic Table, i.e., N, O, or F. With a few exceptions, usually involving fluorine, the associated energies are less than 20-25 kcal mol^{-1}. Hydrogen bonds may be inter or intramolecular". This definition is limited to an

already classical conception of this specific molecular interaction. It does not embrace cases such as a π-electron systems as proton acceptors, charge-assisted H-bonds of the OHO^+ and OHO^- type. Moreover, in cases of strong H-bonds, a covalent nature of interaction is revealed (Sobczyk et al., 2005).

According to the simple valence bond theory, a hydrogen atom should be capable of forming only one chemical bond. In any cases, however, hydrogen is formally two-valent. According to Pauling`s definition "under certain conditions an atom of hydrogen is attracted by rather strong forces to two atoms, instead of only one, so that it may be considered to be acting as a bond between them. This additional bond is called hydrogen bond. Pauling also states that the hydrogen bond "is formed only between the most electronegative atoms". In this sense, the terms typical hydrogen bond or conventional hydrogen bond are related to the Pauling definition. There is a variety of typical H-bonds, for example, O-H···O existing for water dimer and formic acid dimer. The following model is useful to illustrate this definition:

$$R_1 - A^{\delta-} - H^{\delta+} \cdots B - R_2$$

where ***A*** and ***B*** are more electronegative atoms than the hydrogen atom. Most often A and B contain $2p_z$ type electrons, and hence, they may be conjugated with R_1 and R_2, if they are π-electron systems.

The atoms in the Periodic Table with electronegativity greater than that of hydrogen are C, N, O, F, P, S, Cl, Se, Br, and I; and hydrogen bonds involving all of these elements are known. On the other hand "π" hydrogen bonds involve an interaction between particularly positive hydrogen and the electrons in a double and triple bond. Atoms with electronegativity greater than hydrogen have the capability of forming A-H···B hydrogen bonds if B has an unshared pair of electrons, but in some cases the interaction is so weak that most chemists consider that there is no hydrogen bond formed. However, in the second half of the last century, evidence has gradually accumulated that hydrogen bonds other than the conventional hydrogen bond are ubiquitous. These include CH···*n* hydrogen bonds (*n* is lone pair electrons, as contrasted to π; CH···O, CH···N, etc., 2-4 kcal mol^{-1}) and XH··· π hydrogen bonds (X = O, N, etc., 2-4 kcal mol^{-1}).

In H-bonds, the same forces are manifested as in other molecular interactions. Those forces are electrostatic in nature. However, one can distinguish a few specific features that make it possible to discriminate H-bond complex from the universal van der Waals associates and electron-donor-acceptor, named usually charge transfer complex. The most applicable is a geometric criterion. When the H-bond is compared with the van der Waals interaction, the equilibrium distance between H and B atoms is dramatically different. In the case of van der Waals interactions, the distance between H and B is close to the sum of van der Waals radii, whereas in the most frequently observed O-H···O bridges range between 1.6 and 2.2 Å, while from summing the H (~1.2 Å) and O (~ 1.52 Å) van der Waals radii, one obtains for $R_{H\cdots O}$ approximately 2.7 Å. Thus, a great shortening is observed.

2.2 Hydrogen bonds in carboxylic compounds

The specific interaction via H-bond is manifested in several physical properties of systems. Infrared and Raman spectroscopic evidence for hydrogen bonding is the shift of the A–H stretch in a molecule toward lower frequencies. Accordingly, infrared spectroscopy has been very important in hydrogen bonding investigations. Spectra of a hydrogen bond system

present broader, more intense and shifted bands than non-hydrogen bonded systems (Emsley, 1980). The broad envelope bands region could be used to classify hydrogen bonds. In infrared spectra, broad envelope bands in 1800–900 cm^{-1} region are an evidence of short hydrogen bonds (O···O distance of 2.4–2.5 Å). In compounds with medium (O···O distance of 2.5–2.8 Å) and weak (O···O distance of 2.8–3.0 Å) hydrogen bonds, these broad envelopes appear in 3500–2000 cm^{-1} region (Gonzalezsanchez, 1958). The phenomena observed in IR absorption spectra related to stretching ν(AH), γ(AH), and δ(AH) bending vibrations are characteristic for this kind of interaction.

Undoubtedly, these phenomena are due to the changes in charge distribution, which may be related to electron delocalization. Because both heavy-atoms components usually contain orbital able to conjugate with π-electrons systems (np orbitals or similar ones) the IR spectroscopy gives some indirect information about π-electron delocalization. The behavior of H-bonded systems in IR spectra is explained through a decrease of the force constant of ν(AH) vibrations, which leads to stronger coupling with low frequency modes and coupling of Fermi resonance type, an increase of the polarizability of the H-bond. A decrease of the force constant of ν(AH) vibrations and an increase of the force constants of δ(AH) and γ(AH) vibrations are caused by polarization of the AH bond and a shift of the proton toward the proton acceptor. For supramolecular polymeric structures formed by O-H···O hydrogen bonds, the most important spectral region is that related to medium and weak HB (Chagas et al., 2008). In this kind of structures the bands in this region are more broad and enveloped than solids with discrete HB. Figure 1 shows the infrared spectra of some compounds that present medium and weak extended HB, when the envelope bands are observed at 3500-2000 cm^{-1} region (Chagas et al., 2008; Diniz et al., 2002).

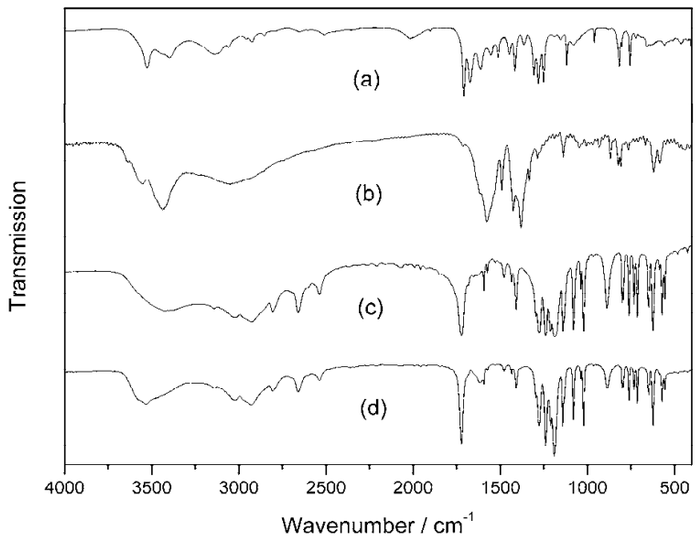

Fig. 1. Infrared spectra of compounds with extended HB: a) 1,2,4,5-benzenetetracarboxylic acid, b) triaquacopper(II) 1,2,4,5-benzenetetracarboxylate tetrahydrate, c) o-sulfobenzoic acid and d) hexaaquazinc(II) hydrogen o-sulfobenzoate.

Infrared spectra of hydrate compounds generally show some broad and intense envelope bands in the range of hydrogen-bond (HB) modes. In contrast, the water modes are very weak in Raman spectra. As a result of this, the Raman spectra of hydrate compounds are

usually better than infrared spectra (Diniz et al., 2002). In compounds that present short O-H···O HB, two bands in Raman spectra are observed: one around 300 cm^{-1} assigned to symmetric stretching mode of OH···O group and around 850 cm^{-1} assigned to the asymmetric one. The O-H stretching mode is observed around 2500 cm^{-1}. In extended structures, the bands assigned as stretching mode of D-H···A group (where D is the donor atom of HB and A is the acceptor of HB) appear at 3100 and 2400 cm^{-1} and bands related to deformation modes at 1650-1620 cm^{-1} region and around 1160 cm^{-1}. In solid state investigation of aminopyridinium derivatives (Lorenc et al., 2008a; Lorenc et al., 2008b) the extended HB were identified by single-crystal X-ray diffraction and by Raman and Infrared spectra. Bands related to stretching modes as so as deformation modes of NH···O, NH···N and OH···O groups were observed in vibrational spectra, as can be seen in Table 1. These results confirm the capability of these technics in studies of supramolecular HB in solid state samples.

APBS[a]			AP[a]			ACP[b]			ACPSe[b]			Assignment
IR	R	Calc.	IR	R	Calc.	IR	R	Calc.	IR	R	Calc.	
3351	-	3542	3445	3447	3467	3456	3454	3562	3351	-	3545	ν(NH···O)
						3297	3298	3444	3288	3317		ν_{as}(NH···O)
						3233			3243	3191	3175	ν_{s}(NH···O)
2860								3672	2900-2600	2474	2719 2275	ν(OH···O)
	1674						1640		1663 1647 1623	1652 1627	1661 1648 1622	δ(NH···O)
			1490 1443									δ(NH···N)
									1004	1001	1009	γ(O···HN)
										450	474	ν(O···HO)

[a] (Lorenc et al., 2008b), [b] (Lorenc et al., 2008a). APBS = 2-aminopyridinium-4-hydroxybenzenosulfonate, AP = 2-aminopyridine, ACP = 2-amino-5-chloropyridine, ACPSe = 2-amino-5-chloropyridinium hydrogen selenate.

Table 1. Supramolecular hydrogen bond vibrations in aminopyridinium derivatives.

3. Antihypertensive drugs and Raman spectra

Hypertension is one of the most prevalent diseases worldwide affecting millions of people (Brandão et al., 2010). Hypertension occurs when blood pressure levels are above the reference values for the general population. Several groups of drugs are used to combat high blood pressure as the carboxypeptidase enzyme inhibitors and the diuretics.

The chlortalidone (CTD) and hydrochlorothiazide (HYD) diuretics drugs are widely used in hypertension treatment. These drugs are active pharmaceutical ingredients with long-acting oral activity. The CTD has two polymorphic forms described in the literature, form I and form III, respectively (Martins et al., 2009), although the HYD has only one single-

crystal structure reported in literature (Dupont and Dideberg, 1972). The enalapril carboxypeptidase enzyme inhibitor drug presents a low solubility which difficult their absorption by human body. Due to this fact the drug is administered as enalapril maleate (ENM), which is a compound more soluble than the enalapril itself. The crystal structure of the ENM drug was described for Précigoux (Precigoux et al., 1986). Another drug very common in hypertension treatment is the losartan potassium (LOS), which is an angiotensin II receptor (type AT1) antagonist (Erk, 2001). In hypertension treatment is common the use of two (or more) drug in association with diuretics. All of these compounds can be used in association and structural and vibrational descriptions of them are show below. The molecular structure and Raman spectra of these drugs are displayed in Figures 2 and 3, respectively. The assignment of the selected bands are listed in Table 2 and marked in Figure 3.

The Raman spectrum of the CTD drug presents vibrational modes of functional groups of CTD molecule, such as stretching modes of NH (3251 cm^{-1}), CO_{amide} (1657 cm^{-1}), SO (1163 cm^{-1}) and CCl (682 cm^{-1}) bonds (Nakamoto, 1986). The ν(NH), ν(SO), ν(CCl) in the Raman spectrum of the HYD drug occur at 3266, 1166 and 610 cm^{-1}, respectively. These bands were used to identify this drug in the associations (Nakamoto, 1986). In ENM drug, bands in the region of 3054 to 2891 cm^{-1} were observed in the Raman spectrum of this compound which can be assigned as ν(CH) of aromatic ring, symmetric and asymmetry stretching modes of CH_2 and CH_3 groups. Other bands as carbonyl stretching of amide, carbonyl stretching of maleate and carbonyl stretching of ester were also observed (Widjaja et al., 2007). For LOS, the most important bands are observed at 807 and 819 cm^{-1} assigned to imidazole ring deformation and at 1489 cm^{-1} attributed to N=N stretching mode (Raghavan et al., 1993).

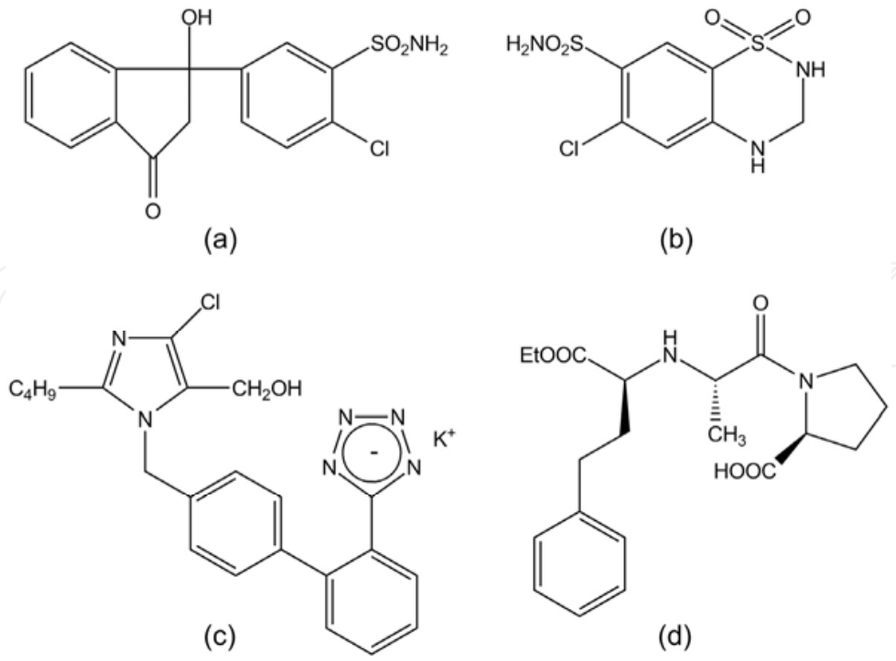

Fig. 2. Chemical structure of a) chlortalidone, b) hydrochlorothiazide, c) losartan potassium and d) enalapril.

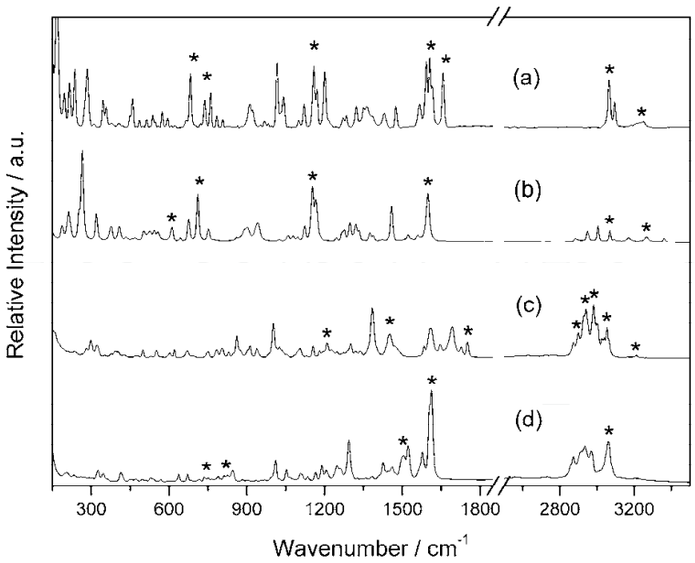

Fig. 3. Raman spectra of a) chlortalidone, b) hydrochlorothiazide, c) enalapril maleate and d) losartan potassium. The * represent the most important bands.

Mode	Compounds			
	CTD	HYD	ENM	LOS
ν(CCl)	682	610		
γ(CH)	761	710	751	761
$\Phi_{imidazole\ ring}$				810
δ(CH)	1156			
ν(SO)	1163	1166		
ν(CCO)			1210	
$\delta_{sym}(CH_2)$			1451	
ν(N=N)				1498
ν(CC)	1567	1552		1616
$\nu(CO)_{maleate}$			1584	
δ(NH)	1605	1602		
$\nu(CO)_{amide}$	1657		1648	
$\nu(CO)_{enalapril}$			1730	
$\nu(CO)_{ester}$			1750	
$\nu(CH_3)$ and $\nu(CH_2)_{aliphatic}$			2890-2980	2950-2870
ν(CH)	3063	3069	3054	3064
ν(NH)	3251	3266	3212	

sym and asym: symmetric and asymmetric modes; δ: in plane bending; γ: out of plane bending.

Table 2. Experimental Raman frequencies for chlortalidone, hydrochlorothiazide, enalapril maleate and losartan potassium drugs.

3.1 Polymorphism and vibrational spectra

In solid pharmaceuticals compounds is very common the occurrence of polymorphism phenomena, which may change physical properties of the compounds; e.g., solubility, melting point, optical and electrical properties, density, hardness and conductivity (Dunitz and Bernstein, 1995). The solubility is one of the most important factors in the drugs absorption, once the modification of this property can change the bioavailability. It may bring serious problems for the patients and for the pharmaceutical industries. For example, in investigation about mebendazole drug (Ferreira et al., 2010), that is used in treatment of worms infestations, three polymorphic forms called A, B and C were identified. The main difference in their physical-chemical properties is the water solubility that modifies the therapeutics effect of these polymorphs. The form A is more soluble and stable than forms B and C. However, the C form is more efficacious in comparison to B form. Other interesting example occur with ritonavir drug, which is a protease inhibitor of human immunodeficiency virus type 1 (HIV-1) and used in the treatment of Acquired Immune Deficiency Syndrome (AIDS) (Chemburkar et al., 2000). A more stable polymorph was reported in the literature (form II), which presents serious solubility problems in compared with the original form (form I). This fact brings problems for patients and pharmaceutical industry, which was forced to remove lots of capsules that had form II, from the market (Bauer et al., 2001). In the literature (Chemburkar et al., 2000) was discussed that the difference between solubility of forms I and II is due to the changes of hydrogen bonds strength in solid state.

Due to this fact, it is very important to identify the presence (or not) of different polymorphic forms in pharmaceuticals formulations. The main technique used in identification of polymorphism is the single-crystal X-Ray diffraction, but due to the difficulty of synthesize this kind of samples, other techniques are used, for example, Raman spectroscopic and X-Ray powder diffraction. Additionally, the Raman spectroscopy may be used in the identification of polymorphism (Raghavan et al., 1993), since different vibration modes can be associated to modifications in molecular packing in crystalline solids. These differences are observed mainly in low-frequency, where may arise lattice vibration that is more sensitive to structural changes in solid state. In this sense, the polymorphism investigation of LOS and CTD will be described in section 3.1.1.

3.1.1 Losartan potassium

Based on aforementioned points an investigation about crystalline phases of antihypertensive LOS by Raman spectroscopy and powder X-Ray is described below. The crystalline forms to LOS drug are described in the literature (Fernandez et al., 2002; Hu et al., 2005b). Figure 4 displays the Raman spectra of two crystalline phases (A and B) for the LOS.

Raman spectrum for sample A is slightly different from sample B spectrum. It can be better see in the region among 950 to 250 cm^{-1} (Figure 4b), where the mainly differences are displayed with asterisk (*). For example, it can be observed that in sample A spectrum the ring breathing mode of the imidazole ring [$\Phi_{imidazole}$] arise at 810 cm^{-1} and the same mode in sample B spectrum appears at 813 cm^{-1}. Apart this, in sample A the band associated to C-H out of plane mode of the biphenyl ring [γ(C-H)] is observed as a shoulder at 761 cm^{-1} and in sample B this band appears at 765 cm^{-1} as a single band.

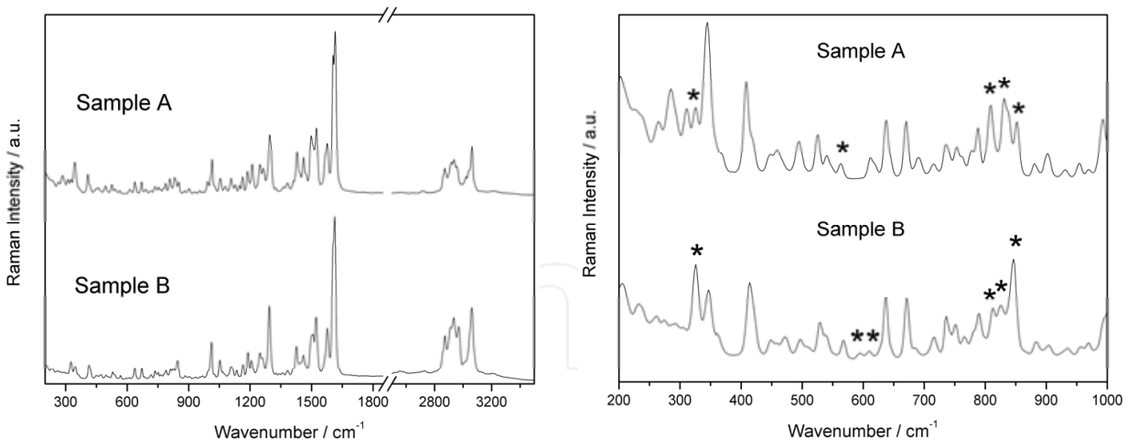

Fig. 4. Raman spectra of a) two crystalline phases (samples A and B) losartan potassium and b) a region of 200 to 1000 cm^{-1}.

The X-ray powder diffraction data is in agreement with Raman data, which may be observed in Figure 5, where the samples present different crystalline forms. The peak fitting suggests that the sample A crystallizes in orthorhombic system (Pbca), with unit cell parameters of a = 13.1389(3) Å, b = 25.6885(5) Å, c = 31.1822(7) Å (Hu et al., 2005a). It was observed that the compound is a pseudo-polymorph, due to the presence of the seven water molecules in its unit cell that also contains two potassium cations and two LOS anions. This structure is stabilized by medium and weak hydrogen bond (OH···N and OH···O) (Hu et al., 2005a). For sample B the Bragg`s peak did not fit to any described phases in the literature for this drug. Vibrational and diffraction data of samples A and B suggested that the differences between these two polymorphic forms may be due to differences in intermolecular interaction and crystal symmetry. Thus, the association of Raman spectroscopy and X-ray powder diffraction data can provide a better description of phase analyses in solid pharmaceutical formulations.

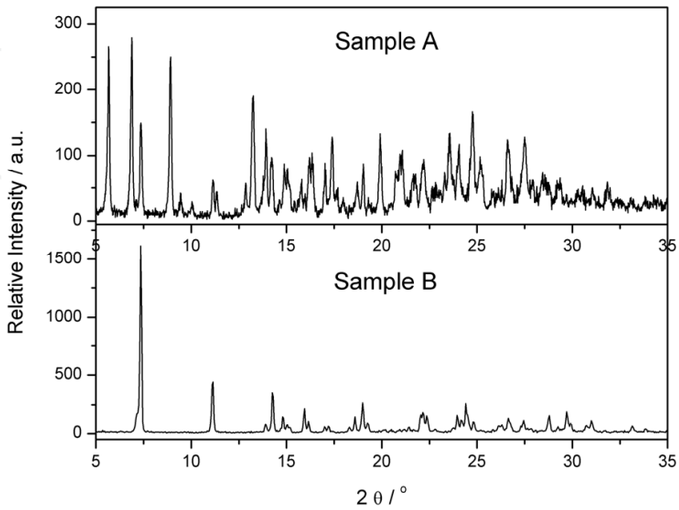

Fig. 5. X-ray powder diffractogram of two samples (A and B) of losartan potassium.

3.1.2 Chlortalidone

The association of computational methodologies and experimental techniques has become in the last few years an essential tool to completely comprehend supramolecular systems (Yan et al., 2007). The wide variety of interactions that rule these systems and their complexity deserve a more detailed analysis in order to describe and to foresee their physical-chemical properties. The computational methods have been rapidly developed in such a way that now it is possible to study systems that some years ago were enviable. For example, Seiffert and co-workers have performed an extended work about the polymorphs structures of lithium-boron imidazolates (Baburin et al., 2011). They have analyzed 30 different structures concerning the potential capability of hydrogen storage of these species.

The effect of the polymorphism in pharmacological science is quite important in the bioavailability, since it can affect physical properties such as solubility and stability of the compound (Yamada et al., 2011). The effects of the polymorphic form on the performance, stability and efficacy of the pharmacological forms have been widely investigated (Brittain, 2009, 2010). The CTD (Figure 2a) presents three different polymorphs forms, but only two of them already have their crystallographic structure known (forms I and III). In this way we have performed density functional theory (DFT) calculations in order to analyze these two distinct species of CTD.

The theoretical investigation of the polymorphs structures of CTD was carried out with periodic density functional theory (DFT) calculations employing the LDA approximation according to Perdew-Zunger (PZ) functional. The wave functions of valence electrons are shown by a plane wave basis set with maximum kinetic energy of 30 hartree (60 Ry). The optimization process was taken using a grid with 2 x 2 x 2 *k* points. The starting geometries for those calculations were the crystallographic data (Martins et al., 2009). All the calculations were performed in the Quantum Espresso (Baroni et al.) (PWscf) program package. The geometries were fully optimized including the atomic coordinates and the lattice parameters. The calculations of vibrational frequencies at the Γ point, were performed on the optimized geometry. These vibrational frequencies are quite useful since they can be used to help in the experimental attributions of the bands in infrared spectrum (De Abreu et al., 2009).

In Figure 6 are shown the optimized structures for the CTD polymorphs I (Fig. 6a) and III (Fig. 6b). It is interesting to note in these figures that both structures are stabilized through hydrogen bonds forming a network in three dimensions. In form I it can be observed the formation of a dimmeric structure in an 8 membered ring through the NH···OC/OC···HN atoms. In this same polymorph there is another hydrogen bond formed between the OH···OC groups. In form III there are two different hydrogen bonds stabilizing the supramolecular structure, one involving the groups OH···OC, like in form I, and another with the NH_2 ···OC groups, that it is not present in form I. Table 3 contains the experimental and theoretical crystal data for both forms. One can note that there was a contraction in the estimated crystal axis of both polymorphs compared to experimental, the difference is about 2 – 7%. The angles are also well described presenting an error bar of -2 – 1% that represents an expansion and contraction, respectively. The crystallographic parameter that suffered the biggest deviance was the unit cell volume that showed an error about 10 and 12% to forms I and III, respectively. However these changes in the crystallographic parameters did not modify the symmetry of the solid (monoclinic system).

	Form I		Form III	
	Experimental	Calculated	Experimental	Calculated
a / Å	6.2270(2)	6.0227	7.9957(2)	7.8520
b / Å	8.3870(3)	8.1662	8.1467(2)	7.7988
c / Å	14.3640(4)	13.8537	11.4761(3)	10.7156
α / °	92.141(2)	91.6952	80.448(2)	80.861
β / °	101.050(2)	101.583	79.277(2)	79.527
γ / °	107.024(2)	108.088	86.106(2)	87.652
V / Å^3	700.50(4)	631.40	723.77(3)	637.02

[a]Experimental data taken from (Martins et al., 2009). [b]Theoretical values calculated in this work.

Table 3. Experimental[a] and theoretical[b] crystal data for chlortalidone forms I and III.

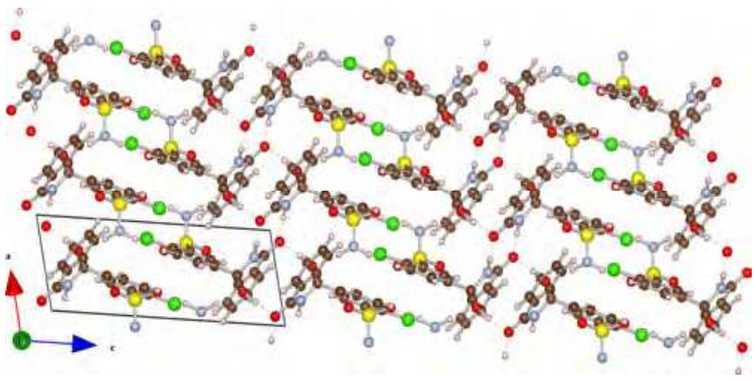

(a)

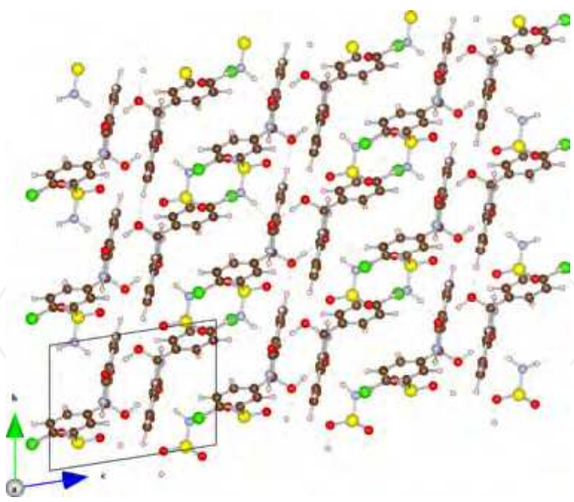

(b)

Fig. 6. Optimized structures of the chlortalidone polymorphs I (a) and III (b).

Concerning the energetics of these species, form I is about 84 kcal mol^{-1} more stable than form III, if we taking into account only the electronic energy. This energetic difference is probably due to the presence of more intermolecular interactions in form I than in III. Table 4 presents the experimental and theoretical infrared attribution for the polymorphs I and III

of CTD. The main vibrational modes related to the intramolecular hydrogen bonds were chosen in a tentative to distinguish the two species. In form I the N-H group is involved in the dimmer formation through a hydrogen bond interaction, it is evidenced by the shift to higher wavenumbers, from 3000 cm^{-1} to 3181 cm^{-1} of the stretching mode of N-H group. The same behavior is observed in the ν (O-H) mode that is shifted from 2861 cm^{-1} to 2968 cm^{-1}, as can be seen in table 4. The formation of intermolecular hydrogen bonds in form III can be evidenced if one compares the shift in the ν (O-H) and ν (NH···O) calculated modes. It is important to mention that in high frequency is observed the biggest deviations from the experimental values.

	Experimental	Theoretical	
Mode	Form I	Form I	Form III
ν(S-NH_2)	918	931	946
ν(S-O)	1165	1154	1276
ν(N-H)	3259	3000	3181
ν(O-H)	2858	2861	2968
ν(C=O)	1681	1670	1647
ν(C-OH)	1043	1042	1063
ν(N-H_2)	3259	3200	3110 / 3117
ν(NH...O)	3550		
ν(NH...O)as	3280	2942, 2998	3008 / 3031
ν(NH…O)s	3240		
ν(OH...O)	2720	2861	2968 / 2988
δ (NH...O)	1600	1628	1635
δ (O...HN)	1000	-	-

Table 4. Experimental (form I) and theoretical infrared attributions of the chlortalidone forms I and III. Wavenumbers are in cm^{-1}.

3.2 Association of hypertensive drugs

3.2.1 Lorsatan potassium in association with chlortalidone and hydrochlorothiazide

To the bands identification, these pharmaceuticals were mixed in a stoichiometric proportion (1:1), (1:2), (4:1), (2:1). It is important emphasize that the calculation of the different proportions was made using the minimum dosage of the associations that is 50 mg for LOS and 12.5 mg for diuretics. Before analyses of these associations, it is necessary know the main Raman bands of the diuretics, since they are used in minimum dosage in pharmaceuticals associations when compared with LOS.

Figures 7 and 8 display the characteristic bands of the LOS/CTD and LOS/HYD associations in the different proportions. It can be observed in the (1:1) rate characteristic bands of the CTD, Figure 7a, at 3094 and 1657 cm^{-1}. The same bands were observed in the rates (1:2) and (1:4). Moreover for (1:2) and (1:4) can be also observed the bands at 3250, 1474, 909, 759, 682 and 460 cm^{-1}. The difference is due to the fact that relative intensity in 1:4 is bigger than in 1:2. However, when for association where LOS increase, 2:1 rate, only one band assigned to CTD drug is verified at 1657 cm^{-1} (Figure 7d). On the other hand, in the 4:1 rate (Figure 7e) the profile of the spectrum is characteristic of LOS drug.

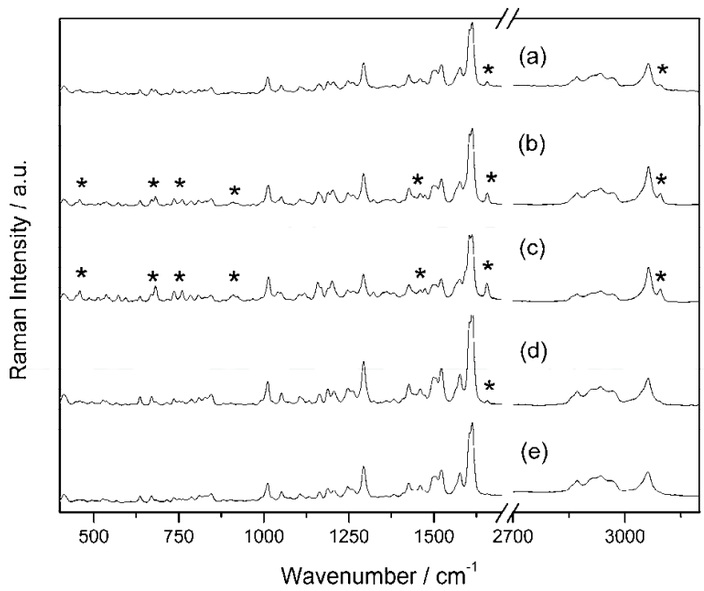

Fig. 7. Raman spectra of losartan potassium in association to chlortalidone in proportions: a) 1:1, b) 1:2, c) 1:4, d) 2:1 and e) 4:1.

Similar results are observed for association with LOS and HYD. Figure 8 shows the Raman spectra of this association. It can be observed that in the rate 1:1 (Figure 8a), just one band was assigned to the presence of HYD at 3005 cm^{-1}. For 1:2 and 1:4 rates (Figures 8b and 8c) were verified bands at 3361, 3268, 3170, 3005, 1320, 1152, 902 and 601 cm^{-1}, characteristics of the HYD. The main different between them is that in 1:4 rate, the relative intensity is bigger than 1:2 rate. In the 2:1 rate the characteristic band of the HYD was observed at 3005 cm^{-1} (Figure 8d) and for the 4:1 proportion the entire spectrum is characteristic of the LOS (Figure 8e).

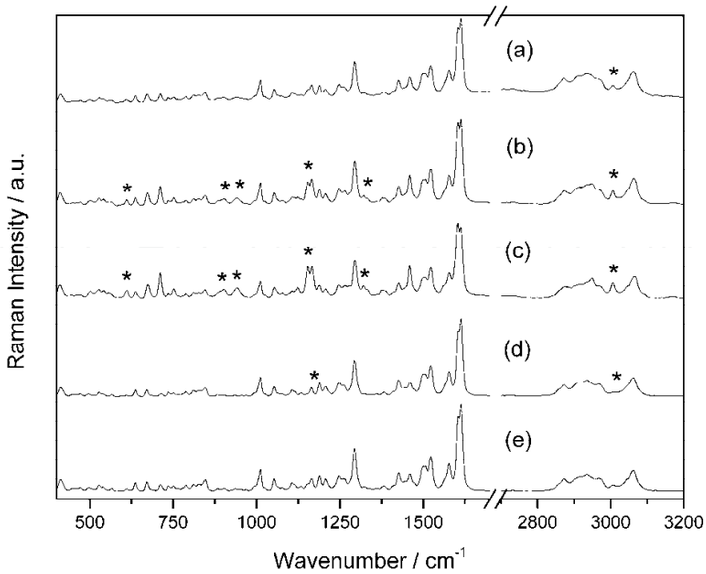

Fig. 8. Raman spectra of losartan potassium in association to hydrochlorothiazide in proportions: a) 1:1, b) 1:2, c) 1:4, d) 2:1 and 4:1.

The optimization of this fast and simple method of analyze is important, mainly in antihypertensive drugs associations. These results show the potential of Raman spectroscopy in qualitative analysys in the pharmaceutical associations, however when the LOS is in large proportions, like in 4:1 rate, occur the overlapping between the bands of pharmaceutical formulations and it is not possible characterized the diuretics bands.

3.2.2 Enalapril maleate in association with chlortalidone and hydrochlorothiazide

The Raman spectra of the ENM/CTD and ENM/HYD associations are shown in Figures 9 to 14. The proportions of the drugs at the associations were 1:2.5, 1.6:1 and 2:1. The proportions respected the minimum dosage of each drug what is 12.5 mg for CTD and HYD and 5 mg for ENM (Brandão et al., 2010).

Figure 9c shows the Raman spectrum of the ENM/CTD association in proportion 1:2.5 (1 mg of ENM for 2.5 mg of CTD). In this Raman spectrum all characteristic bands of the CTD drug are present and have relative intensities larger those characteristic bands of the ENM drug. This is due to the large quantity of the CTD drug in the mixture. Some bands of the ENM are not present in the Raman spectra of the association obtained.

In Raman spectrum of the ENM and CTD association in proportion 1.6:1 (1.6 mg of ENM for 1 mg of CTD) shown in Figure 10c are observed characteristic bands of the ENM and CTD drugs. The relative intensities of the characteristic bands of CTD drug were reduced due to lower proportion of this drug in the mixture.

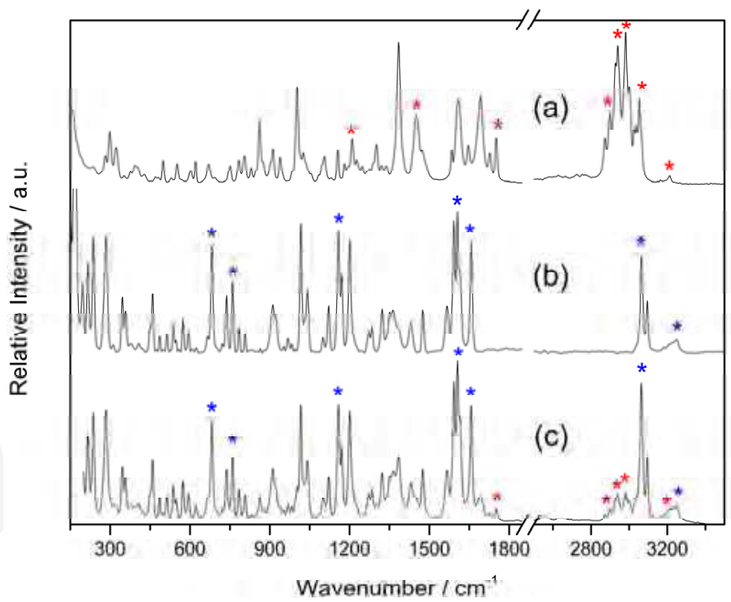

Fig. 9. Raman spectra of the (a) enalapril maleate, (b) chlortalidone and (c) enalapril maleate and chlortalidone association in proportion 1:2.5. The symbol * refers to bands relative to enalapril maleate vibrations and * the bands relative to chlortalidone vibrations.

Figure 11c shows the Raman spectrum of the ENM and CTD association in proportion 2:1 (2 mg of ENM for 1 mg of CTD). This spectrum is very similar to that showed in Figure 10c. The characteristic bands of the ENM and CTD drugs are observed being that the relative intensities of the CTD bands are smaller than ENM. This similarity between these spectra refers to almost equal proportion of drugs in the mixtures.

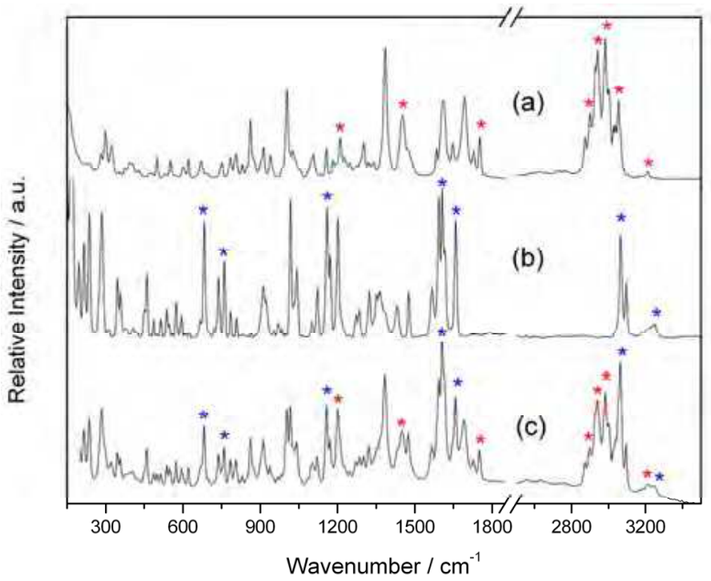

Fig. 10. Raman spectra of the (a) enalapril maleate, (b) chlortalidone and (c) enalapril maleate and chlortalidone association in proportion 1.6:1. The symbol * refers to bands relative to enalapril maleate vibrations and * the bands relative to chlortalidone vibrations.

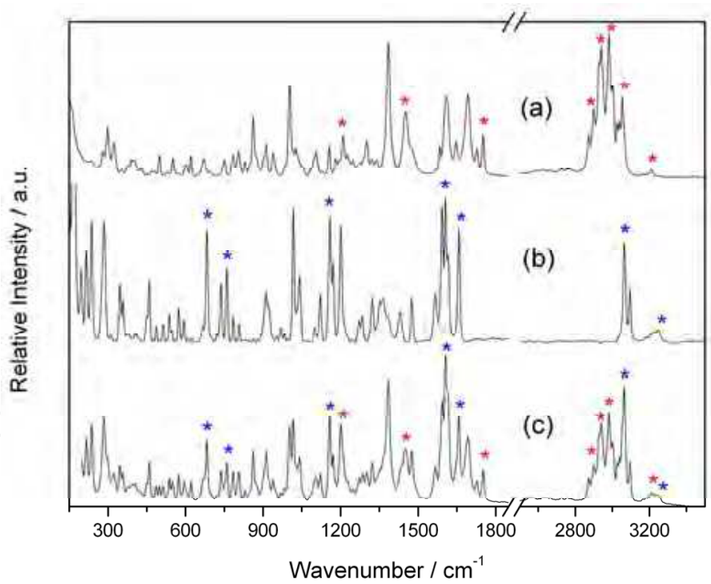

Fig. 11. Raman spectra of the (a) enalapril maleate, (b) chlortalidone and (c) enalapril maleate and chlortalidone association in proportion 2:1. The symbol * refers to bands relative to enalapril maleate vibrations and * the bands relative to chlortalidone vibrations.

Figure 12c shows the Raman spectrum of the ENM/HYD association in proportion 1:2.5 (1 mg of ENM for 2.5 mg of HYD). In this Raman spectrum all characteristic bands of the HYD drug are present and have relative intensities larger than the characteristic bands of the ENM drug. Similar to the ENM/CDT, this is due to the large quantity of the HYD drug in the mixture. Some bands of the ENM are not present in the Raman spectra of associations.

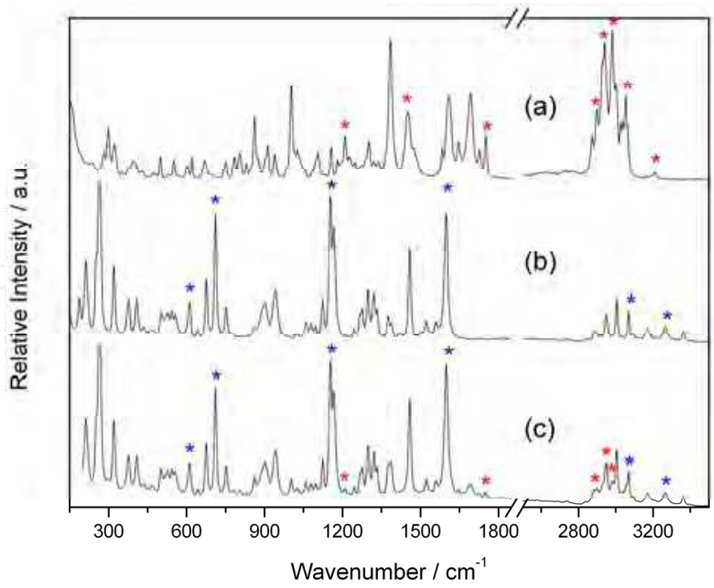

Fig. 12. Raman spectra of the (a) enalapril maleate, (b) hydrochlorothiazide and (c) enalapril maleate and hydrochlorothiazide association in proportion 1:2.5. The symbol * refers to bands relative to enalapril maleate vibrations and * the bands relative to hydrochlorothiazide vibrations.

In Raman spectrum of the ENM/HYD association in proportion 1.6:1 (1.6 mg of ENM for 1 mg of HYD) shown in Figure 13c are observed characteristic bands of the ENM and HYD drugs. The relative intensities of the characteristic bands of HYD drug such as ν(NH), ν(SO) and γ(CH) were reduced due to the lower proportion of this drug in the mixture.

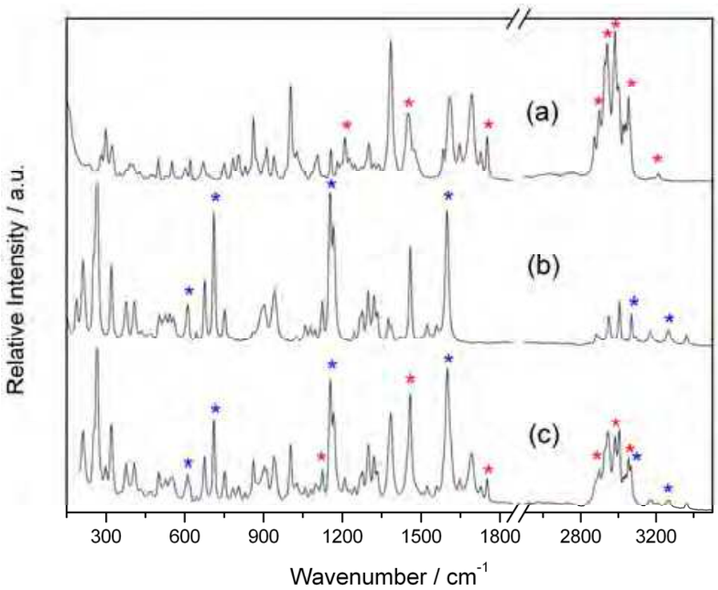

Fig. 13. Raman spectra of the (a) enalapril maleate, (b) hydrochlorothiazide and (c) enalapril maleate and hydrochlorothiazide association in proportion 1.6:1. The symbol * refers to bands relative to enalapril maleate vibrations and * the bands relative to hydrochlorothiazide vibrations.

Figure 14c shows the Raman spectrum of the ENM and HYD association in proportion 2:1 (2 mg of ENM for 1 mg of HYD). The characteristic bands of the ENM and HYD drugs are observed being that the relative intensities of HYD bands are smaller than ENM band intensities.

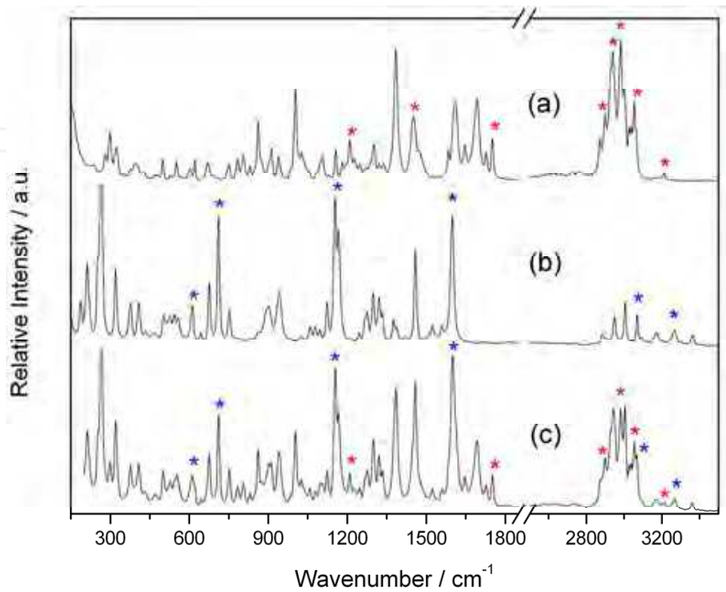

Fig. 14. Raman spectra of the (a) enalapril maleate, (b) hydrochlorothiazide and (c) enalapril maleate and hydrochlorothiazide association in proportion 2:1. The symbol * refers to bands relative to enalapril maleate vibrations and * the bands relative to hydrochlorothiazide vibrations.

4. Conclusion

These results show the potential of Raman spectroscopy in the identification of polymorphism in pharmaceuticals as well in the qualitative analyze in drugs associations. Additionally, the combination of these results with X-ray diffraction and theoretical calculations data complete the description of the solid state, in special in supramolecular chemistry investigations.

5. Acknowledgment

The authors are thankful to the Brazilian Agencies CAPES, FAPEMIG, CNPq for the financial support, LabCri (Instituto de Física – Universidade Federal de Minas Gerais) and LDRX (Instituto de Física – Universidade Federal Fluminense) for X-ray facilities, and Filipe B. de Almeida and Chris H. J. Franco for help in infrared and Raman spectra.

6. References

Aaltonen, J., Gordon, K.C., Strachan, C.J., Rades, T. (2008). Perspectives in the use of spectroscopy to characterise pharmaceutical solids. *International Journal of Pharmaceutics*, Vol. 364, No 2, pp. (159-169), 0378-5173

Baburin, I.A., Assfour, B., Seifert, G., Leoni, S. (2011). Polymorphs of lithium-boron imidazolates: energy landscape and hydrogen storage properties. *Dalton Transactions*, Vol. 40, No 15, pp. (3796-3798), 1477-9226

Baroni, S., dalCorso, A., deGironcoli, S., Giannozzi, P., Cavazzoni, C. *http://www.democritos.it*

Bauer, J., Spanton, S., Henry, R., Quick, J., Dziki, W., Porter, W., Morris, J. (2001). Ritonavir: An Extraordinary Example of Conformational Polymorphism. *Pharmaceutical Research*, Vol. 18, No 6, pp. (859-866), 0724-8741

Brandão, A.A., Magalhães, M.E.C., Ávila, A., Tavares, A., Machado, C.A., Campana, E.M.G., Lessa, I., Krieger, J.E., Scala, L.C., Neves, M.F., Silva, R.C.G., Sampaio, R. (2010). VI Diretrizes Brasileiras de Hipertensão. *Arquivos Brasileiros de Hipertensão*, Vol. 95, No (11 - 17), 0066-782X

Brittain, H.G. (2009). Polymorphism and Solvatomorphism 2007. *Journal of Pharmaceutical Sciences*, Vol. 98, No 5, pp. (1617-1642), 0022-3549

Brittain, H.G. (2010). Polymorphism and Solvatomorphism 2008. *Journal of Pharmaceutical Sciences*, Vol. 99, No 9, pp. (3648-3664), 0022-3549

Carlucci, L., Ciani, G., Proserpio, D.M. (2003). Polycatenation, polythreading and polyknotting in coordination network chemistry. *Coordination Chemistry Reviews*, Vol. 246, No 1-2, pp. (247-289), 0010-8545

Chagas, L.H., Janczak, J., Gomes, F.S., Fernandes, N.G., de Oliveira, L.F.C., Diniz, R. (2008). Intermolecular interactions investigation of nickel(II) and zinc(II) salts of ortho-sulfobenzoic acid by X-ray diffraction and vibrational spectra. *Journal of Molecular Structure*, Vol. 892, No 1-3, pp. (305-310), 0022-2860

Chemburkar, S.R., Bauer, J., Deming, K., Spiwek, H., Patel, K., Morris, J., Henry, R., Spanton, S., Dziki, W., Porter, W., Quick, J., Bauer, P., Donaubauer, J., Narayanan, B.A., Soldani, M., Riley, D., McFarland, K. (2000). Dealing with the Impact of Ritonavir Polymorphs on the Late Stages of Bulk Drug Process Development. *Organic Process Research & Development*, Vol. 4, No 5, pp. (413-417), 1083-6160

De Abreu, H.A., Junior, A.L.S., Leitao, A.A., De Sa, L.R.V., Ribeiro, M.C.C., Diniz, R., de Oliveira, L.F.C. (2009). Solid-State Experimental and Theoretical Investigation of the Ammonium Salt of Croconate Violet, a Pseudo-Oxocarbon Ion. *Journal of Physical Chemistry A*, Vol. 113, No 23, pp. (6446-6452), 1089-5639

Diniz, R., de Abreu, H.A., de Almeida, W.B., Sansiviero, M.T.C., Fernandes, N.G. (2002). X-ray crystal structure of triaquacopper(II) dihydrogen 1,2,4,5-benzenetetracarboxylate trihydrate and Raman spectra of Cu2+Co2+, and Fe2+ salts of 1,2,4,5-benzenetetracarboxylic (pyromellitic) acid. *European Journal of Inorganic Chemistry*, Vol., No 5, pp. (1115-1123), 1434-1948

Dunitz, J.D., Bernstein, J. (1995). Disappearing Polymorphs. *Accounts of Chemical Research*, Vol. 28, No 4, pp. (193-200), 0001-4842

Dupont, L., Dideberg, O. (1972). Structure cristalline de l'hydrochlorothiazide, C7H8ClN3O4S2. *Acta Crystallographica Section B*, Vol. 28, No 8, pp. (2340-2347), 0567-7408

Emsley, J. (1980). VERY STRONG HYDROGEN-BONDING. *Chemical Society Reviews*, Vol. 9, No 1, pp. (91-124), 0306-0012

Erk, N. (2001). Analysis of binary mixtures of losartan potassium and hydrochlorothiazide by using high performance liquid chromatography, ratio derivative

spectrophotometric and compensation technique. *Journal of Pharmaceutical and Biomedical Analysis*, Vol. 24, No 4, pp. (603-611), 0731-7085

Fernandez, D., Vega, D., Ellena, J.A., Echeverria, G. (2002). Losartan potassium, a non-peptide agent for the treatment of arterial hypertension. *Acta Crystallographica Section C-Crystal Structure Communications*, Vol. 58, No (m418-m420), 0108-2701

Ferreira, F.F., Antonio, S.G., Rosa, P.C.P., Paiva-Santos, C.d.O. (2010). Crystal structure determination of mebendazole form A using high-resolution synchrotron x-ray powder diffraction data. *Journal of Pharmaceutical Sciences*, Vol. 99, No 4, pp. (1734-1744), 1520-6017

Gonzalezsanchez, F. (1958). INFRA-RED SPECTRA OF THE BENZENE CARBOXYLIC ACIDS. *Spectrochimica Acta*, Vol. 12, No 1, pp. (17-33),

Hoeben, F.J.M., Jonkheijm, P., Meijer, E.W., Schenning, A. (2005). About supramolecular assemblies of pi-conjugated systems. *Chemical Reviews*, Vol. 105, No 4, pp. (1491-1546), 0009-2665

Hu, X.-R., Wang, Y.-W., Gu, J.-M. (2005a). Losartan potassium 3.5-hydrate, a new crystalline form. *Acta Crystallographica Section E*, Vol. 61, No 9, pp. (m1686-m1688), 1600-5368

Hu, X.R., Wang, Y.W., Gu, J.M. (2005b). Losartan potassium 3.5-hydrate, a new crystalline form. *Acta Crystallographica Section E-Structure Reports Online*, Vol. 61, No (M1686-M1688), 1600-5368

Kollman, P.A., Allen, L.C. (1972). THEORY OF HYDROGEN-BOND. *Chemical Reviews*, Vol. 72, No 3, pp. (283-&), 0009-2665

Lorenc, J., Bryndal, I., Marchewka, M., Kucharska, E., Lis, T., Hanuza, J. (2008a). Crystal and molecular structure of 2-amino-5-chloropyridinium hydrogen selenate - its IR and Raman spectra, DFT calculations and physicochemical properties. *Journal of Raman Spectroscopy*, Vol. 39, No 7, pp. (863-872), 0377-0486

Lorenc, J., Bryndal, I., Marchewka, M., Sasiadek, W., Lis, T., Hanuza, J. (2008b). Crystal and molecular structure of 2-aminopyridinium-4-hydroxybenzenosulfonate - IR and Raman spectra, DFT calculations and physicochemical properties. *Journal of Raman Spectroscopy*, Vol. 39, No 5, pp. (569-581), 0377-0486

Martins, F.T., Bocelli, M.D., Bonfilio, R., de Araujo, M.B., de Lima, P.V., Neves, P.P., Veloso, M.P., Ellena, J., Doriguetto, A.C. (2009). Conformational Polymorphism in Racemic Crystals of the Diuretic Drug Chlortalidone. *Crystal Growth & Design*, Vol. 9, No 7, pp. (3235-3244), 1528-7483

Nakamoto, K. (1986). *Infrared and Raman Spectra of Inorganic and Coordination Compounds* (4th), John Wiley & Sons, 0471010669, New York

Precigoux, G., Geoffre, S., Leroy, F. (1986). N-(1-Ethoxycarbonyl-3-phenylpropyl)-l-alanyl-l-prolinium-hydrogen maleate (1/1), enalapril (MK-421). *Acta Crystallographica Section C*, Vol. 42, No 8, pp. (1022-1024), 0108-2701

Raghavan, K., Dwivedi, A., Campbell Jr, G.C., Johnston, E., Levorse, D., McCauley, J., Hussain, M. (1993). A Spectroscopic Investigation of Losartan Polymorphs. *Pharmaceutical Research*, Vol. 10, No 6, pp. (900-904), 0724-8741

Sobczyk, L., Grabowski, S.J., Krygowski, T.M. (2005). Interrelation between H-bond and Pi-electron delocalization. *Chemical Reviews*, Vol. 105, No 10, pp. (3513-3560), 0009-2665

Takahashi, O., Kohno, Y., Nishio, M. (2010). Relevance of Weak Hydrogen Bonds in the Conformation of Organic Compounds and Bioconjugates: Evidence from Recent

Experimental Data and High-Level ab Initio MO Calculations. *Chemical Reviews*, Vol. 110, No 10, pp. (6049-6076), 0009-2665

Wang, K., Duan, D., Wang, R., Liu, D., Tang, L., Cui, T., Liu, B., Cui, Q., Liu, J., Zou, B., Zou, G. (2009). Pressure-Induced Phase Transition in Hydrogen-Bonded Supramolecular Adduct Formed by Cyanuric Acid and Melamine. *Journal of Physical Chemistry B*, Vol. 113, No 44, pp. (14719-14724), 1520-6106

Widjaja, E., Lim, G.H., Chow, P.S., Tan, S. (2007). Multivariate data analysis as a tool to investigate the reaction kinetics of intramolecular cyclization of enalapril maleate studied by isothermal and non-isothermal FT-IR microscopy. *European Journal of Pharmaceutical Sciences*, Vol. 32, No 4-5, pp. (349-356), 0928-0987

Yamada, H., Masuda, K., Ishige, T., Fujii, K., Uekusa, H., Miura, K., Yonemochi, E., Terada, K. (2011). Potential of synchrotron X-ray powder diffractometry for detection and quantification of small amounts of crystalline drug substances in pharmaceutical tablets. *Journal of Pharmaceutical and Biomedical Analysis*, Vol. 56, No 2, pp. (448-453), 0731-7085

Yan, S., Lee, S.J., Kang, S., Lee, J.Y. (2007). Computational approaches in molecular recognition, self-assembly, electron transport, and surface chemistry. *Supramolecular Chemistry*, Vol. 19, No 4-5, pp. (229-241), 1061-0278

Ye, B.H., Tong, M.L., Chen, X.M. (2005). Metal-organic molecular architectures with 2.2 '-bipyridyl-like and carboxylate ligands. *Coordination Chemistry Reviews*, Vol. 249, No 5-6, pp. (545-565), 0010-8545

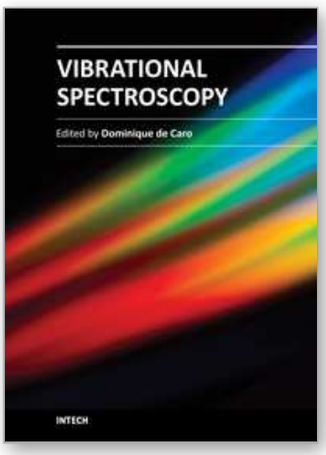

Vibrational Spectroscopy

Edited by Prof. Dominique De Caro

ISBN 978-953-51-0107-9
Hard cover, 168 pages
Publisher InTech
Published online 24, February, 2012
Published in print edition February, 2012

The infrared and Raman spectroscopy have applications in numerous fields, namely chemistry, physics, astronomy, biology, medicine, geology, mineralogy etc. This book provides some examples of the use of vibrational spectroscopy in supramolecular chemistry, inorganic chemistry, solid state physics, but also in the fields of molecule-based materials or organic-inorganic interfaces.

How to reference

In order to correctly reference this scholarly work, feel free to copy and paste the following:

Luciano H. Chagas, Márcia C. De Souza, Weberton R. Do Carmo, Heitor A. De Abreu and Renata Diniz (2012). Structure Characterization of Materials by Association of the Raman Spectra and X-Ray Diffraction Data, Vibrational Spectroscopy, Prof. Dominique De Caro (Ed.), ISBN: 978-953-51-0107-9, InTech, Available from: http://www.intechopen.com/books/vibrational-spectroscopy/structure-characterization-of-materials-by-association-of-the-raman-spectra-and-x-ray-diffraction-da

INTECH
open science | open minds

InTech Europe
University Campus STeP Ri
Slavka Krautzeka 83/A
51000 Rijeka, Croatia
Phone: +385 (51) 770 447
Fax: +385 (51) 686 166
www.intechopen.com

InTech China
Unit 405, Office Block, Hotel Equatorial Shanghai
No.65, Yan An Road (West), Shanghai, 200040, China
中国上海市延安西路65号上海国际贵都大饭店办公楼405单元
Phone: +86-21-62489820
Fax: +86-21-62489821

IntechOpen